

Two-step field-induced singlet dissociation in a fluorene trimerJ. Cabanillas-Gonzalez,* M. R. Antognazza, T. Virgili, and G. Lanzani
IFN-CNR, Dipartimento di Fisica, ULTRAS-INFM, Politecnico di Milano, Milano 20133, Italy

C. Gadermaier

Christian-Doppler Laboratory Advanced Functional Materials, Institut für Festkörperphysic, Tech. Univ. Graz, Petersgrasse 16, 8010 Graz, Austria

M. Sonntag and P. Strohriegl

Lehrstuhl Makromolekulare Chemie I, Universität Bayreuth, 95440 Bayreuth, Germany

(Received 9 September 2004; revised manuscript received 13 December 2004; published 26 April 2005)

We time resolve the event of singlet separation into free carriers in an oligofluorene using femtosecond field assisted pump-probe technique. Steady state photoinduced absorption (PA) measurements have also been employed to identify triplet absorption (T_1-T_n) in the spectral region of 1.8 eV. As a result of an applied electric field of 2.2 MV/cm singlets are observed to undergo a dissociation process consisting of first singlet splitting into bound polaron pairs and second further dissociation of polaron pairs into free carriers. Subsequent free carrier recombination yields a new population of singlets and triplets. Our results suggest that nongeminate recombination leads to the formation of 35% singlets and 65% triplets.

DOI: 10.1103/PhysRevB.71.155207

PACS number(s): 78.47.+p, 39.30.+w, 34.70.+e

I. INTRODUCTION

Conjugated polymers have attracted considerable attention as active materials for solar cells and photodiodes.¹⁻³ For this reason, understanding the carrier photogeneration process in these materials becomes not only a fundamental question but also a technological demand. There are two main descriptions proposed to explain the mechanism of carrier photogeneration under the action of an applied electric field. According to the 1-D semiconductor description, e-h pairs undergo directly on-chain dissociation into free carriers.^{4,5} This theory however does not consider excitonic effects nor disorder broadening, which have been proved to be important in noncrystalline organic semiconductors.⁶ Within the molecular framework, carrier generation requires the formation of intermediate charge transfer (C-T) states or polaron pairs and their subsequent separation into free carriers. Polaron-pair formation may proceed via on-chain thermalization assisted by vibrational relaxation,⁷ via interchain exciton diffusion towards lower energy sites⁸ or even due to partial dissociation induced by the electric field.^{9,10} The resulting geminate pairs remain bounded by the Coulombic interaction and free carrier generation takes place only in the presence of an applied electric field. Alternately, polaron pairs will recombine forming new singlet states. Competition between both processes determines the overall carrier photogeneration efficiency.

Poly(9,9-dioctylfluorene) (PFO) and related polyfluorene structures have attracted great attention in the past few years due to their beneficial properties for LED and solar cell design.¹¹⁻¹³ Polaron-pair photogeneration in PFO has been understood as a sequential excitation process towards upper lying energy states, leading to exciton on-chain dissociation in time scales of less than 150 fs.¹⁴ Electric field pump-probe experiments performed in PFO have demonstrated that free carriers are generated directly from splitting of singlets in

subpicosecond time scales.¹⁵ Hereby, sequential resonant excitation or intrachain relaxation assisted by an electric field could be responsible for the formation of free carriers in these ultrafast time scales. Similar observations have been reported in a methyl substituted ladder-type poly(paraphenylene) (*m*-LPPP), where field assisted dissociation of singlets into free carriers proceeds directly without any signature of intermediate states.¹⁶ In *m*-LPPP, however, carrier population builds up for approximately 2 ps suggesting a dissociation process influenced by exciton migration during interchain thermalization.

We present electric field pump-probe measurements on a fluorene trimer. In this short π -conjugated system, ultrafast on-chain dissociation is prevented. By exciting at the tail of absorption with moderate pump fluences we intend to minimize sequential excitation. Moreover, its short conjugation length and diffusion-limited exciton motion should lead to a slower singlet relaxation allowing therefore to resolve in time a gradual free carrier generation process. By studying a fluorene trimer we intend to provide a simplified picture of the carrier photogeneration process which can be applied to more complicated polymeric structures. We show evidences for polaron pairs as a precursor species of free carriers.

II. EXPERIMENTAL DETAILS

The fluorene trimer employed in this work was synthesized by means of a Suzuki cross-coupling reaction described elsewhere.¹⁷ Films for optical measurements were deposited by spin coating a 20 g/l solution of trimer in chloroform with a spin speed of 2000 rpm over glass substrates. Samples for field assisted pump-probe measurements consisted of single layer LEDs fabricated from films spun over indium tin oxide (ITO) substrates with aluminum cathodes deposited on top by thermal evaporation. CW-PA measure-

ments were performed using as excitation the 351.1 nm and 363.8 nm output of an argon ion coherent innova multiline laser chopped at 9 Hz. A 200 W halogen lamp provided the light source for transmission measurements. The sample was kept in vacuum (10^{-4} mbar) and measurements were performed at approximately 100 K. Light transmitted through the sample was detected using a photodiode and lock-in amplifier referred to as the chopping frequency. Pump-probe and electric field pump-probe measurements were carried out using the 780 nm 150 fs pulses at 1 KHz and 750 μ J per pulse provided by a Kerr-lens mode locked Ti: Sapphire laser with chirped pulse amplification. The output was split in pump and probe beams. The pump beam was doubled in frequency and focused on one pixel through the ITO side. The resulting 390 nm pump beam assured excitation below the localization threshold of the trimer. The probe was temporally delayed respect to the pump, sent to a sapphire plate to generate white light and spatially overlapped with the pump beam on the pixel. A photodiode with an interferometer filter placed in front provided wavelength selective detection of the light reflected by the cathode. For optical pump-probe measurements frequency modulated detection was achieved by chopping the pump at 470 Hz and detecting with a lock-in amplifier referred to as the same frequency. For electric field assisted pump-probe measurements, a reverse square profile electric field of 2.2 MV/cm with a frequency of 470 Hz was applied to the device, using for detection the same phase-sensitive scheme. The obtained signal ($\Delta^2 T/T$) correspond to the field induced changes on the differential transmission ($\Delta T/T$) given by $\Delta^2 T/T = (\Delta T/T)_F - \Delta T/T$. An interpretation of the sign of $\Delta^2 T/T$ is done as follows. Whether $\Delta T/T$ is positive (stimulated emission or photobleaching), $\Delta^2 T/T$ positive means an increase in population induced by the field whereas $\Delta^2 T/T$ negative leads to field induced quenching. The opposite situation holds for $\Delta T/T$ negative.

III. RESULTS

A. Absorption, photoluminescence, and CW-photoinduced absorption

The shape of the absorption and photoluminescence (PL) spectra of the trimer clearly resembles PFO being both spectra shifted to higher energies. The trimer possesses a broad absorption band centered at 3.6 eV and PL spectrum with vibronic replica at 2.6, 2.8, 2.9 and 3.1 eV (Fig. 1). The chemical structure of the trimer (inset Fig. 1) is characterized by three fluorene units with short dialkylated side chains. This substitution leads to glassy morphologies revealed from the presence of a glass transition temperature at around 114 °C and the absence of melting and crystallization points provided by differential scanning calorimetry (DSC) scans.¹⁷ The CW-PA spectrum of the trimer, (displayed in Fig. 2), is dominated by a sharp peak around 1.8 eV with vibronic replica at higher energies. No evidences are found for infrared vibronic side bands characteristic of sub-bandgap transitions in charged species¹⁸ so that we assign the PA band to triplet state absorption in agreement with similar findings in PFO.¹² The full width half maximum of the PA

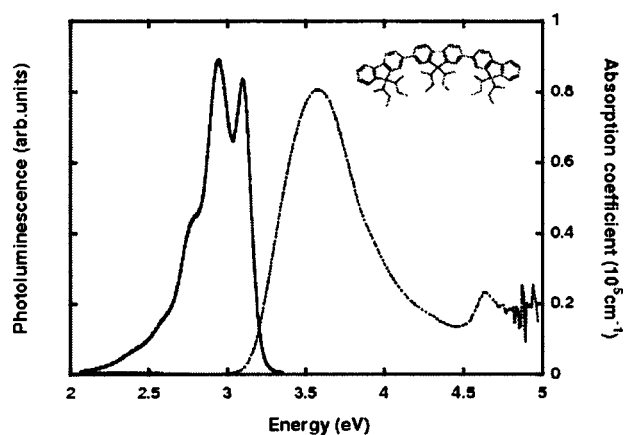


FIG. 1. Absorption (dotted line) and PL (solid line) spectra of 9,9,9',9',9''-Hexa-sec-butyl-[2,2';7',2'']terfluorene. The chemical structure is shown in the inset figure.

band is 133 meV. The inset of Fig. 3 displays the power dependence at the maximum of the PA signal. The dependence obeys a linear law suggesting a preferential monomolecular recombination channel. Figure 3 depicts the frequency dependence of the PA signal. The decay of the triplet PA fits well a two lifetime decay of the type

$$\Delta T \propto \frac{A}{\sqrt{1 + (2\pi f \tau_1)^2}} + \frac{B}{\sqrt{1 + (2\pi f \tau_2)^2}}, \quad (1)$$

where f is the chopping frequency, τ_1 and τ_2 the decay lifetimes and A and B hold for the percentage of triplets that decay with lifetimes τ_1 and τ_2 , respectively. From the fit of the experimental data we obtain that 4% of the triplets decay with a lifetime of 2 ms and 96% with a lifetime of 24 ms. A predominant decay lifetime of 1.8 ms was found before in spun films of PFO although in this case 13% of the triplets were observed to decay with a much shorter decay component of 98 μ s.¹⁹ It has been discussed that triplet photogeneration may proceed in certain polymers by geminate recombination of long-lived polaron pairs due to evolution of

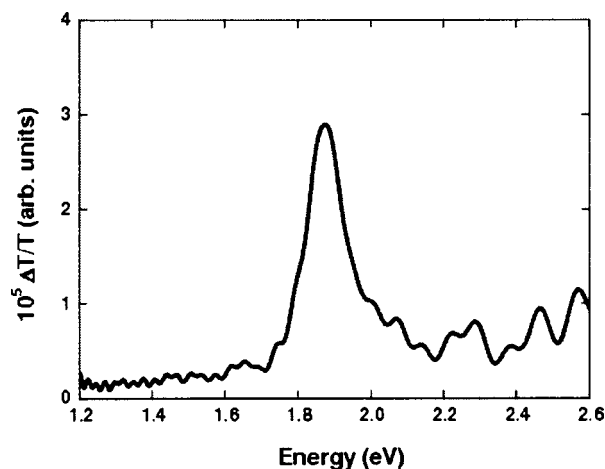


FIG. 2. CW-PA spectrum of the trimer pumping with 25 mW and detecting at 9 Hz.

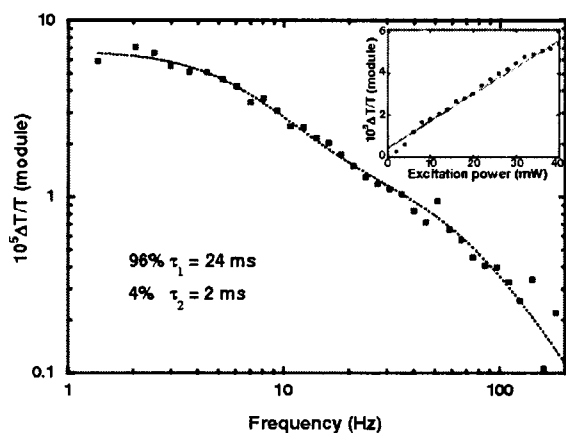


FIG. 3. Dependence of the triplet PA signal upon the modulation frequency pumping with an output power of 25 mW. The experimental data (filled squares) was fitted with two different decay components. The inset figure displays the power dependence of the PA signal for a constant modulation frequency of 9 Hz.

their spin states.²⁰ In PFO, however, this hypothesis is discarded due to its low polaron quantum yield. Hereby, inter-system crossing of thermalized singlets is therefore the dominant triplet generation mechanism.²¹

B. Optical pump-probe dynamics

The chirp free differential transmission spectra at different delay times is shown in Fig. 4. At 1 ps delay time, the spectrum is characterized by a region of stimulated emission (SE) over 2.5 eV and a PA band (PA₁) which extends from 1.4 eV until nearly 2.5 eV. According to findings in PFO it seems reasonable to assign this band to S_1-S_n excited state absorption.²² At 400 ps after photoexcitation only a broadband centered around 2.2 eV is observable (PA₂). The dynamics of SE, PA₁ and PA₂ are depicted in Fig. 5. The SE and PA₁ decay dynamics follow parallel trends while a slower decay component is observed for PA₂. Moreover, the dynamics of PA₂ are found to be independent with the power excitation (Fig. 6), pointing towards monomolecular recombination. The dominance of a monomolecular recombination

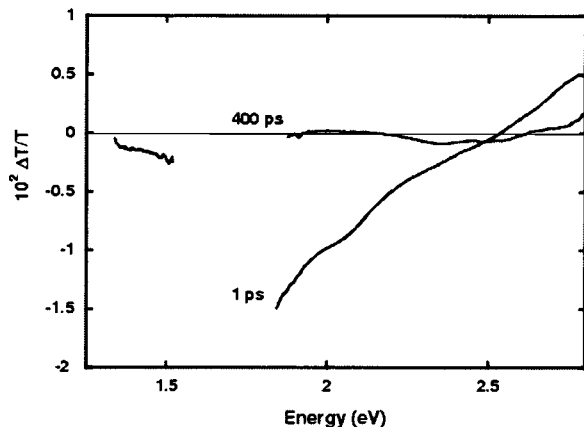


FIG. 4. Transient absorption spectrum of the trimer at 1 ps and 400 ps pump-probe delay.

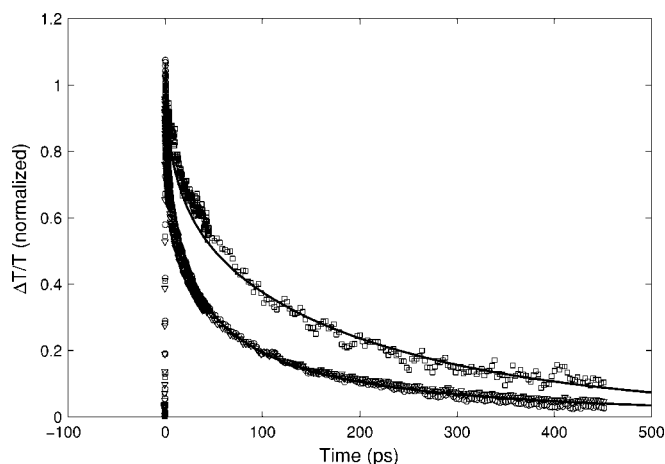


FIG. 5. Normalized pump-probe dynamics at 1.5 eV (circles), 2.2 eV (squares) and 2.7 eV (triangles). The dynamics at 1.5 eV and 2.2 eV were both fitted to stretched exponentials (bold lines). From the fit parameters we estimate the decay rates for singlets and polaron pairs to be $0.11 \times t^{-0.6}$ and $4 \times 10^{-3} \text{ ps}^{-1}$, respectively.

channel is characteristic of geminate recombination of polaron pairs. Polaron-pair generation in the trimer could be a process where only one photon is involved. This hypothesis is partially supported by the linear dependence of the initial $\Delta T/T$ value at 2.2 eV with the pump fluence. Accordingly, polaron-pair photogeneration could take probably place via interchain thermalization of the photogenerated singlets followed by their subsequent dissociation.²³ We should remark, however, that at 2.2 eV, polaron-pair absorption overlaps with the PA₁ band, so that singlet excited state may also contribute to the total $\Delta T/T$ value. The linear dependence of $\Delta T/T$ with the power intensity could therefore be influenced by generation of singlets as well as polaron pairs.

C. Electro-optical pump-probe dynamics

The electric field pump-probe dynamics at three characteristic energies, namely, 2.2 eV (polaron pairs), 1.8 eV

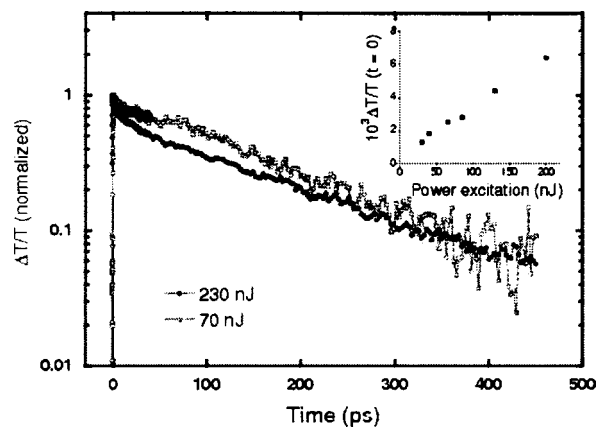


FIG. 6. A comparison between the dynamics of polaron pairs at two different power intensities: 230 nJ (circles) and 70 nJ (squares). The inset figure depicts the linear dependence of the differential transmission value at zero time delay upon power excitation.

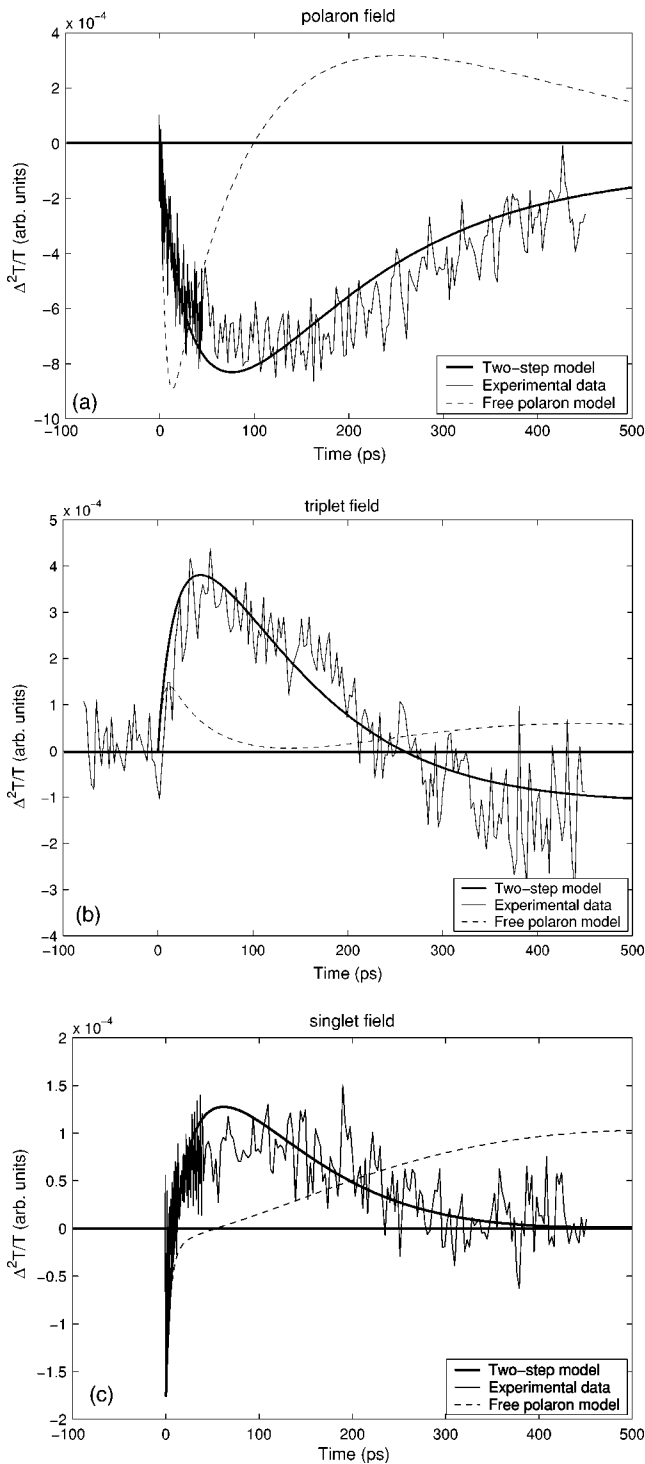


FIG. 7. Electric field pump-probe dynamics at (a) 2.2 eV, (b) 1.8 eV and (c) 1.5 eV. The experimental data (straight line) were fitted using two different models: free polaron model (dotted line) and two-step model (bold line).

(singlets/triplets) and 1.5 eV (singlets) are depicted in Figs. 7(a)–7(c), respectively. The field induced dissociation of singlets into charged species is confirmed by two observations. First, the positive rise of $\Delta^2 T/T$ at 1.5 eV [Fig. 7(c)], in time scales of approximately 100 ps pointing towards singlet quenching ($\Delta T/T_{1.5 \text{ eV}} < 0$). Second, the negative rise of

$\Delta^2 T/T$ at 2.2 eV [Fig. 7(a)], which suggests a new population of charged states generated under the action of the electric field ($\Delta T/T_{2.2 \text{ eV}} < 0$). We should remark here that the electric field applied in reverse bias assures the negligible injection of carriers into the trimer. Beyond 100 ps, $\Delta^2 T/T$ at 2.2 eV and 1.5 eV decays due to charge recombination and singlet regeneration, respectively. Both decay trends show a certain parallelism which indicates a clear link between them. These observations constitute an experimental evidence for the formation of a new singlet population as a result of charge recombination. The early $\Delta^2 T/T$ dynamics at 1.8 eV [Fig. 7(b)], resembles those ascribed to singlets [Fig. 7(c)]. After 250 ps, however, they experience a change of sign followed by a long-lived negative signal, which it does not appear in the singlet dynamics and must therefore be attributed to triplet formation. Since the possibility of inter-system crossing during the first 400 ps can be excluded, triplets can only be harvested by recombination of nongeminate polarons. Accordingly, the presence of free carriers generated from singlet separation and their recombination forming singlets and triplets in a certain ratio is the most likely explanation for the long-lived signal at 1.8 eV. Finally, we should note the negative value of $\Delta^2 T/T$ at zero time delay in Figs. 7(b) and 7(c). On the basis of negligible changes of the cross section induced by the electric field, here $\Delta^2 T/T < 0$ holds strictly for an increase in singlet population. Such a situation would be fulfilled if carriers injected into the trimer recombine generating new singlets. This possibility is rejected since injection under moderate reverse bias is an unlikely scenario. Moreover, the recombination of carriers injected from the opposite sides of the device requires typically time scales of 5 μs in films of PFO,²⁴ inconsistent with the sub-ps induced negative signal. Therefore, the negative signal must be the result of a change in the cross-section values for ground and/or singlet excited absorption induced by the electric field. Since $\Delta^2 T/T$ is negligible at negative time delays, ground state electroabsorption can be ruled out, and the only contribution is due to field induced changes in the excited state absorption cross section. The negative $\Delta^2 T/T$ values suggest in this case a strengthening of the absorption likely induced by the Stark shift of the excited state transitions towards lower energies. Under certain assumptions it is possible to estimate the polarizability of the S_1-S_n transition, which is related to the excited state delocalization. We have reported in other work²⁵ a value for the trimer of $0.43 \times 10^{-19} \text{ eV m}^2/\text{V}^2$ which is approximately 15 times lower than the difference in polarizability between the $1A_g$ and $1B_u$ states of PFO.¹⁹

IV. MODELING AND DISCUSSION

As it has been mentioned in the previous paragraph, the presence of a triplet population harvested from charge recombination is presented as a spectroscopic proof for the nongeminate nature of the charged species. These free carriers could be formed directly from field induced separation of singlets into noncorrelated polarons, as it has been proposed in PFO,¹⁵ or by an indirect process involving intermediate C-T species. According to Arkhipov *et al.*, singlets photo-

generated at low energy sites in *m*-LPPP dissociate into stabilized short off-chain geminate pairs in the presence of an electric field.²⁶ Evolution towards free carriers may be activated by conversion of short geminate pairs into loosely bound long polaron pairs, due to the interaction with long lifetime species such as triplets. In order to identify the mechanisms of charge photogeneration in the trimer, the field induced dynamics were fitted according to two different models which account, respectively, for direct singlet dissociation into free carriers and a two-step indirect dissociation process. We proceed to describe each of the models next.

A. Free polaron model

Under no applied field the only present species are those created by photogeneration, i.e., singlets and polaron pairs. Attending to Fig. 5, photogeneration of these species proceeds in very short time scales within the pulse duration. The equation rates that govern the singlet (N_s) and polaron-pair (N_{pp}) populations in the absence of a field are therefore given by

$$\frac{dN_s}{dt} = -k_1 N_s + k_2 N_{pp}, \quad (2)$$

$$\frac{dN_{pp}}{dt} = -k_2 N_{pp}, \quad (3)$$

where k_1 and k_2 account for the singlet and polaron-pair recombination rates, respectively. The creation term $k_2 N_{pp}$ stands for the recovery of S_1 singlets due to geminate recombination of polaron pairs, (polaron-pair recombination to S_0 was discarded according to the Onsager model²⁷). The values found for k_1 and k_2 from the fit parameters (Fig. 5) are a dispersive rate of $0.11 \times t^{-0.6}$ and $4 \times 10^{-3} \text{ ps}^{-1}$, respectively. In the presence of an electric field, the free polaron model implies a decrease in the singlet and polaron-pair populations attributed to field induced dissociation of both species into free polarons (N_p). Accordingly, the population of singlets under an electric field ($N_s|_F$) will be governed by

$$\frac{dN_s}{dt} \Big|_F = -k_1 N_s|_F + k_2 N_{pp}|_F - J N_s|_F + \beta K_D N_p^2, \quad (4)$$

where the term $-J N_s|_F$ accounts for field induced dissociation of singlets into free polarons with a dissociation rate J and the term $\beta K_D N_p^2$ for the increase in singlet population due to bimolecular free carrier recombination. The terms K_D and β hold, respectively, for the free carrier recombination rate and the singlet-to-triplet formation ratio, respectively. The triplet population will be given by

$$\frac{dN_T}{dt} \Big|_F = (1 - \beta) K_D N_p^2, \quad (5)$$

where the creation term describes the increase in triplet population from free carrier recombination. Polaron pairs are expected to dissociate with larger rate values than singlets, attending to their lower binding energy. The equations that stand for the polaron-pair and free polaron populations under an electric field are

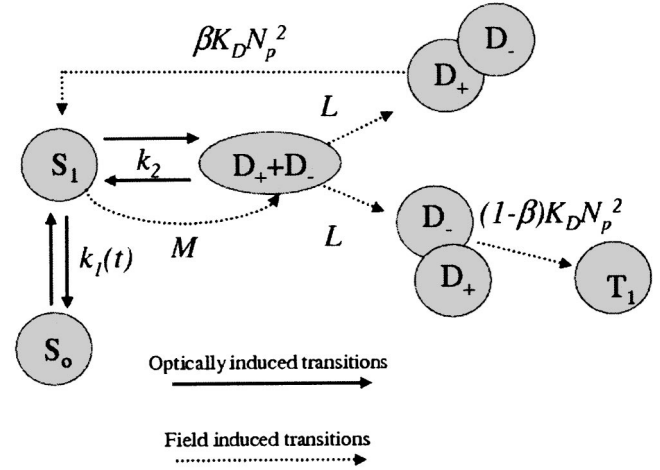


FIG. 8. A scheme of the field induced carrier photogeneration process. Bold arrows refer only to optical induced transitions whereas dashed arrows hold for electric field induced transitions.

$$\frac{dN_{pp}}{dt} \Big|_F = -k_2 N_{pp}|_F - L N_{pp}|_F, \quad (6)$$

$$\frac{dN_p}{dt} \Big|_F = 2L N_{pp}|_F + 2J N_s|_F - K_D N_p^2. \quad (7)$$

Hereby, $-L N_{pp}|_F$ describes the field induced dissociation of polaron pairs into free polarons with a dissociation rate L . The dissociation of singlets and polaron pairs leads to a build-up of free polaron population described by the creation terms $2J N_s|_F$ and $2L N_{pp}|_F$, respectively.

B. Two-step model

The singlet dissociation process underlying this model is a two-step mechanism consisting of (i) splitting of singlets into *stabilized* polaron pairs; and (ii) the further dissociation of polaron pairs into free carriers (see Fig. 8). According to this model, the equation governing the population of singlets under an applied electric field is identical to Eq. (4) with the difference that the destructive term $-J N_s|_F$ accounts this time for singlet dissociation into polaron pairs rather than free polarons. For clarity purposes, we will refer the singlet dissociation rate into polaron pairs as M . We note here that M should be larger than J employed in the last section since Coulombic stabilization involved in polaron pairs leads to a lowering of the energy barrier for dissociation. The polaron-pair population is governed by

$$\frac{dN_{pp}}{dt} \Big|_F = -k_2 N_{pp}|_F + M N_s|_F - L N_{pp}|_F, \quad (8)$$

where a new creation term, $M N_s|_F$, is introduced this time to account for the build-up of polaron pairs from singlet dissociation. The further dissociation of polaron pairs induces a new population of free carriers:

$$\left. \frac{dN_p}{dt} \right|_F = 2LN_{pp}|_F - K_D N_p^2. \quad (9)$$

We remark that free polarons yield only from polaron-pair dissociation with a creation term $2LN_{pp}|_F$. Note the difference respect to Eq. (7), which considers free carrier generation either from singlet as well as polaron-pair dissociation. Free polaron recombination leads again to the recovery of singlets and a new triplet population with a rate equation given by Eq. (5).

C. Discussion

Best fits provided by each model are represented in Figs. 7(a)–7(c). The contributions at different energies from singlets, polaron pairs, free polarons and triplets were statistically weighted by using the appropriate absorption cross-section values for the different transitions involved. The absorption features of polaron pairs and free polarons overlap at 2.2 eV, being undistinguishable with the spectral resolution employed in our experimental setup. The spectral overlap of both species is often reported in other conjugated polymers such as *m*-LPPP^{16,28,29} or blends of 2,5-dioctyloxy poly(*p*-phenylene vinylene) (DOO—PPV) and C60.³⁰ Albeit polaron pairs and free polarons contribute to the fit with similar cross sections, their effects over the dynamics are substantially different according to their recombination behaviors (slow monomolecular for *stabilized* polaron pairs and fast bimolecular for free polarons). Polaron pairs are stabilized by an energy barriers induced by an off-diagonal disorder, i.e., trap states, which reduce their recombination rate. The dynamics at 2.2 eV [Fig. 7(a)], are influenced by singlets, polaron pairs and free polarons. The free polaron model predicts an initial negative signal induced by the generation of free polarons from singlet dissociation. Subsequently, it decays rapidly and changes sign after ~ 80 ps due to fast bimolecular recombination and recovery in singlet population, respectively. Likewise, the two-step model predicts a negative $\Delta^2 T/T$ attributed to singlet dissociation into polaron pairs. In this case, however, charge recombination is delayed by further field induced dissociation of polaron pairs, leading to a gradual increase in free carrier population for the next 70 ps. Beyond these time scales, $\Delta^2 T/T$ decays due to free carrier recombination. It is remarkable that the two-step model predicts a significantly slower signal decay than the free polaron model, which is in good agreement with the experimental data. This effect is attributed to the free carrier populations predicted by each model leading to different bimolecular recombination terms, according to the quadratic dependence with N_p [Eq. (4)]. On the basis of the two-step model, a certain amount of polaron pairs undergo recombination towards S_1 , being therefore lost for free carrier photogeneration. The result is a lower free polaron population which reduces the effects of fast bimolecular recombination. Likewise, the dynamics at 1.8 eV [Fig. 7(b)], and 1.5 eV [Fig. 7(c)] are in good agreement with the predictions of the two-step model, meanwhile the free polaron model underestimates in both cases the quenching signal.

The polaron-pair quantum yield (η_{CT}) and free carrier quantum yield (Ω) can be obtained as $M/(M+k_1)$ and

$L/(L+k_2)$, respectively, from the fit parameters employed in the two-step model. According to this, singlet splitting into polaron pairs accounts for 0.5% of the singlets photogenerated whereas dissociation into free carriers is undergone by 50% of the polaron-pair population. Thereby, the total quantum yield for free carrier generation under a 2.2 MV/cm electric field is given by the product of both quantities, namely, 0.25%. This value is remarkably lower than 3% found in PFO under similar applied fields.¹⁵ The reduced carrier quantum yield observed in the trimer is therefore the result of a competition established between two processes: polaron-pair recombination, with a decay rate given by k_2 , and polaron-pair dissociation, with a dissociation rate L . We should remark that in PFO, field assisted dissociation is likely influenced by on-chain relaxation of nonthermalized excited singlet states. Concerning the oligomer, on-chain dissociation is inhibited since the molecule size is below the typical Coulomb capture radius of 10 nm. Interchain relaxation via exciton migration towards lower energy sites is expected to play a more significant role. The negligible polaron population at zero time delay and its rise extending over 50 ps suggest a slow mechanism of exciton relaxation, likely motivated by the low mobility of excitons photogenerated at the *bottom of the density of states*. These energy sites act as traps which allow the formation of *stabilized* polaron—pairs prior to their dissociation into free carriers due to the continuous action of the electric field.

Note that the two-step model implies a polaron-pair quantum yield which depends on the magnitude of the electric field, in clear disagreement with the Onsager model.²⁷ We remark, however, that the field dependent generation of C-T states is predicted by other models such as the Noolandi-Hong model, proposed for photoconductors.⁹ Moreover, it has been reported that polaron pairs could also play an important role in the mechanism of free carrier recombination in PFO. In this polymer it has been proposed that singlet dissociation into free carriers is immediately followed by Coulomb capture of nongeminate pairs forming an intermediate polaron pair, which subsequently recombines geminately towards a singlet or triplet, depending on its spin nature.¹⁵ This hypothesis has been proposed as an explanation for the high microscopic free carrier mobility derived from the nongeminate recombination rate and the Langevin theory. However, this argument is only valid when the density of free carriers is so high that the average free electron-hole distance is below the Coulomb capture radius. The low excitation densities employed in this study allow ruling out such a possibility, so that we assume that free carriers recombine directly into singlets and triplets.

Taking into account the recombination of free polarons we deduce a value for the singlet-to-triplet formation ratio of 0.35. This value is in reasonable agreement with the 0.25 expected in a spin uncorrelated recombination process and differs significantly from the values reported in PFO (0.7–0.8).^{15,31} Different singlet-to-triplet formation ratios in polymers and monomers have been understood as due to the influence of the exchange interaction in the event of electron hole recombination. In systems with extended π conjugation, the Coulomb capture radius is shorter than the conjugation length, and electron-hole spin interaction takes place through

the overlap of both wave functions.³² Consequently, the recombination process is influenced by the exchange interaction and becomes spin dependent.

V. CONCLUSION

The field induced singlet dissociation process in a fluorene trimer is described as a two-step process consisting of singlet splitting into intermediate *stabilized* polaron pairs and their further dissociation into free carriers. Free carrier generation takes place with a total quantum yield of 0.25%, approximately one order of magnitude lower than in PFO. Subsequent free carrier recombination leads to 35% of singlets and 65% of triplets. The dissociation of singlets pro-

ceeds gradually in the trimer, extending over time scales beyond 50 ps. This result differs notably from what has been reported in PFO, where free carrier generation proceeds in subpicosecond time scales. Such differences are probably motivated by the important role that femtosecond on-chain singlet dissociation plays in long conjugated polymer chains, a mechanism which is prevented in the trimer.

ACKNOWLEDGMENTS

J.C.-G. acknowledges support by the EUROFET (RTN) 5th EU Framework Programme 2002. We thank C. Manzoni and D. Marinotto for technical assistance and L. Lüer for valuable discussions.

*Electronic address: juan.cabanillas@polimi.it; telephone: +39022399 6055; Fax: +39022399 6126.

- ¹N. S. Sariciftci, L. Smilowitz, A. J. Heeger, and F. Wudl, *Science* **258**, 1474 (1992).
- ²G. Yu, J. Gao, J. C. Hummelen, F. Wudl, and A. J. Heeger, *Science* **270**, 1789 (1995).
- ³J. J. M. Halls, A. C. Arias, J. D. MacKenzie, W. Wu, M. Inbasekaran, E. P. Woo, and R. H. Friend, *Adv. Mater. (Weinheim, Ger.)* **12**, 498 (2000).
- ⁴M. C. J. M. Vissenberg and M. J. M. de Jong, *Phys. Rev. Lett.* **77**, 4820 (1996).
- ⁵W. P. Su, J. R. Schrieffer, and A. J. Heeger, *Phys. Rev. Lett.* **42**, 1698 (1979).
- ⁶U. Rauscher, H. Bässler, D. D. C. Bradley, and M. Hennecke, *Phys. Rev. B* **42**, 9830 (1990).
- ⁷V. I. Arkhipov, E. V. Emelianova, and H. Bässler, *Phys. Rev. Lett.* **82**, 1321 (1999).
- ⁸R. Kersting, U. Lemmer, M. Deussen, H. J. Bakker, R. F. Mahrt, H. Kurz, V. I. Arkhipov, H. Bässler, and E. O. Göbel, *Phys. Rev. Lett.* **73**, 1440 (1994).
- ⁹J. Noolandi and K. M. Hong, *J. Chem. Phys.* **70**, 3230 (1979).
- ¹⁰J. Kalinowski, W. Stampor, and P. G. di Marco, *J. Chem. Phys.* **96**, 4136 (1992).
- ¹¹A. W. Grice, D. D. C. Bradley, M. T. Bernius, M. Inbasekaran, W. Wu, and E. P. Woo, *Appl. Phys. Lett.* **73**, 629 (1998).
- ¹²L. C. Palilis, D. G. Lidzey, M. Redecker, D. D. C. Bradley, M. Inbasekaran, E. P. Woo, and W. W. Wu, *Synth. Met.* **121**, 1729 (2001).
- ¹³A. C. Arias, J. D. MacKenzie, R. Stevenson, J. J. M. Halls, M. Inbasekaran, E. P. Woo, D. Richards, and R. H. Friend, *Macromolecules* **34**, 6005 (2001).
- ¹⁴C. Silva, A. S. Dhoot, D. M. Russell, M. A. Stevens, A. C. Arias, J. D. MacKenzie, N. C. Greenham, R. H. Friend, S. Setayesh, and K. Mullen, *Phys. Rev. B* **64**, 125211 (2001).
- ¹⁵T. Virgili, G. Cerullo, C. Gadermaier, L. Lüer, G. Lanzani, and D. D. C. Bradley, *Phys. Rev. Lett.* **90**, 247402 (2003).

- ¹⁶W. Graupner, G. Cerullo, G. Lanzani, M. Nisoli, E. J. W. List, G. Leising, and S. De Silvestri, *Phys. Rev. Lett.* **81**, 3259 (1998).
- ¹⁷M. Sonntag and P. Stohriegel, *Chem. Mater.* **16**, 4736 (2004).
- ¹⁸D. Moses, A. Dogariu, and A. J. Heeger, *Phys. Rev. B* **61**, 9373 (2000).
- ¹⁹A. J. Cadby, P. A. Lane, H. Mellor, S. J. Martin, M. Grell, C. Giebeler, and D. D. C. Bradley, *Phys. Rev. B* **62**, 15 604 (2000).
- ²⁰E. L. Frankevich, A. A. Lymarev, I. Sokolik, F. E. Karasz, S. Blumstengel, R. H. Baughman, and H. H. Hörhold, *Phys. Rev. B* **46**, 9320 (1992).
- ²¹M. Wohlgenannt, W. Graupner, G. Leising, and Z. V. Vardeny, *Phys. Rev. Lett.* **82**, 3344 (1999).
- ²²G. Cerullo, S. Stagira, M. Zavelani-Rossi, S. De Silvestri, T. Virgili, D. G. Lidzey, and D. D. C. Bradley, *Chem. Phys. Lett.* **335**, 27 (2001).
- ²³C. Gadermaier, G. Cerullo, M. Zavelani-Rossi, G. Sansone, G. Lanzani, E. Zojer, A. Pogantsch, D. Beljonne, Z. Shuai, J. L. Brédas, U. Scherf, and G. Leising, *Phys. Rev. B* **66**, 125203 (2002).
- ²⁴M. Redecker, D. D. C. Bradley, M. Inbasekaran, and E. P. Woo, *Appl. Phys. Lett.* **73**, 1565 (1998).
- ²⁵J. Cabanillas-Gonzalez, M. R. Antognazza, T. Virgili, G. Lanzani, M. Sonntag, and P. Stohriegel, *Synth. Met.* (to be published).
- ²⁶V. I. Arkhipov, E. V. Emelianova, and H. Bässler, *Chem. Phys. Lett.* **340**, 517 (2001).
- ²⁷L. Onsager, *Phys. Rev.* **54**, 554 (1938).
- ²⁸W. Graupner, S. Eder, K. Petritsch, G. Leising, and U. Scherf, *Synth. Met.* **84**, 507 (1997).
- ²⁹M. Wohlgenannt, E. J. W. List, C. Zenz, G. Leising, W. Graupner, and Z. V. Vardeny, *Synth. Met.* **116**, 353 (2001).
- ³⁰P. A. Lane, X. Wei, and Z. V. Vardeny, *Phys. Rev. B* **56**, 4626 (1997).
- ³¹M. Wohlgenannt, K. Tandon, S. Mazumdar, S. Ramasesha, and Z. V. Vardeny, *Nature (London)* **409**, 494 (2001).
- ³²J. S. Wilson, A. S. Dhoot, A. J. A. B. Seeley, M. S. Khan, A. Köhler, and R. H. Friend, *Nature (London)* **413**, 378 (2001).